Int J Syst Assur Eng Manag
https://doi.org/10.1007/s13198-021-01269-7

ORIGINAL ARTICLE

Hemorrhage detection using edge-based contour with fuzzy clustering from brain computed tomography images

N. S. Bhadauria[1] · Indrajeet Kumar[2] · H. S. Bhadauria[1] · R. B. Patel[3]

Received: 5 February 2020 / Revised: 17 June 2021 / Accepted: 9 August 2021

Abstract The paper presents a segmentation method for extracting the hemorrhage out of CT (computed tomography) images of brain by using the features of fuzzy clustering together with the level-set segmentation method. The fuzzy clustering is utilized for initialization of level-set function that evolves to extract the desired hemorrhagic region. In addition, the fuzzy clustering has also been utilized for estimating the parameters which control the propagation of level set function. The proposed method eradicates the requirement of manual initialization and re-initialization process which is very much time inefficient, as required by majority of conventional level-set segmentation methods and thus speeding up the process related with evolution of function associated with level-set. The proposed method has been implemented over a dataset containing 300 CT images of brain with hemorrhages of various sizes and shapes and the performance of proposed method is compared with existing techniques like fuzzy c-mean (FCM) clustering and region growing. The results of this method are observed to have highest values related with similarity indices such as overlap metric, accuracy, specificity and sensitivity with values as 87.46%, 85.40%, 98.79% and 79.91% respectively for given dataset of 300 images.

✉ Indrajeet Kumar
ikumar@gehu.ac.in

[1] GBPIET, Pauri Garhwal, Uttarakhand, India

[2] Graphic Era Hill University, Dehradun, India

[3] Chandigarh College of Engineering and Technology, Chandigarh, India

Keywords Computed tomography · Fuzzy clustering · Level set method · Brain hemorrhage

1 Introduction

Brain hemorrhage is a cause of one of the highest deaths following heart diseases and cancer throughout the world. According to the published data in 2018 and Revised in 2021, stroke or brain hemorrhage is one of the highest deaths cause in USA (Heron 2019; Murphy et al. 2021). This escalates the significance of detection of hemorrhage as a primary task to the patients with neurological abnormalities or head injury. It occurs due to bleeding caused by leakage or blood vessels rupturing inside the skull. Computed Tomography (CT) scans are commonly done in order to diagnose the hemorrhage of brain. CT imaging is preferred by the experts due to various reasons involving the reliable way of diagnosing the hemorrhage present in brain, the cost-effectiveness of the imaging, widespread availability, time efficiency along with admirable bony details detection. The visualization of region of abnormalities like hemorrhagic clots found in CT images of brain are dependent of built-in properties such as location, volume, density, relationship between the adjacent composition as well as the technical factors involving slice thickness, scanning angles etc. (Cohen 1992; Praveen et al. 2018). The description of normal brain CT image and haemorrhagic images are shown in Fig. 1. The sample images are taken from dataset which is used for this study.

The identification of hemorrhagic area is very crucial due to its importance in diagnosis and planning related to treatment of hemorrhage. However, because of worst tissue contrast, the identification of hemorrhages using brain CT

Published online: 27 August 2021

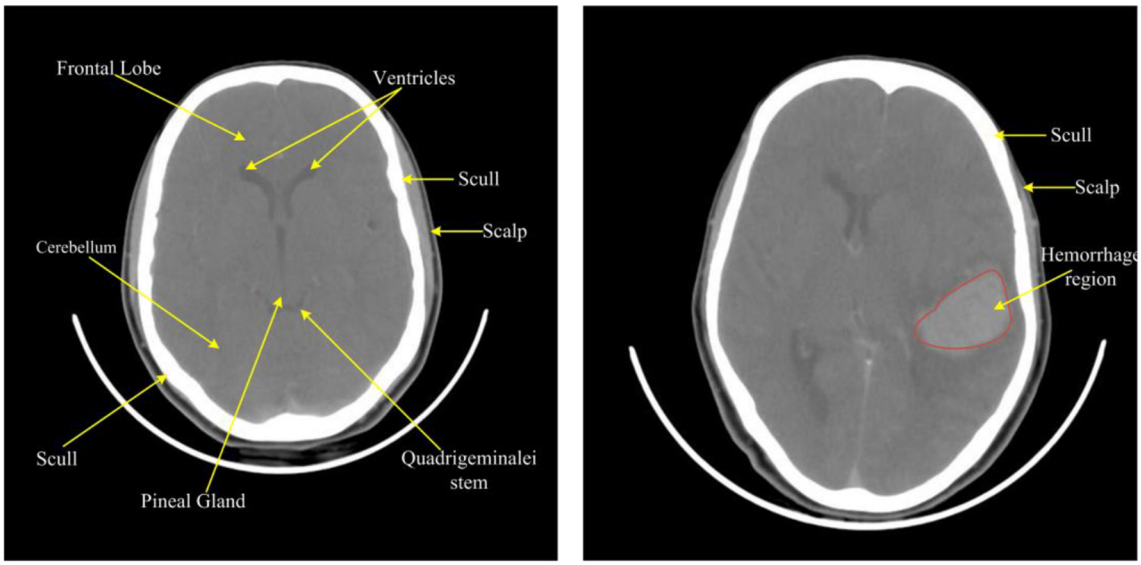

(a) Normal CT image **(b)** CT image having hemorrhage

Fig. 1 Brain CT Image description

images becomes a challenging task (Al-Ayyoub et al. 2013; Gillebert et al. 2014). Various researches are already done on medical image segmentation which mostly involves methods related to fuzzy-set theory, ANNs (Artificial Neural Networks) (Chen et al. 2017), Markov random fields (Zhang et al. 2001) and active contours (Caselles et al. 1993). Presently, in context with medical imaging, approaches based on level-set have also been implemented in various researches given in Sethian (1999); Suri et al. 2002; Yezzi et al. 1997). The segmentation of brain hemorrhage from CT images in studies (Loncaric et al. 1999, 1998) is performed through fuzzy C-mean which is later followed by classification of segmented regions with rule-based methods. Study (Chan 2007) has extracted the regions found with hemorrhage through left–right asymmetry and top-hat transform, which made it capable of detecting small clots of hemorrhage. Bardera et al. (2009) presented a method for segmenting the two basic abnormalities i.e. edema and hemotoma related with the brain, in which segmentation of region with hematoma is done through region growing and that of edema through level set. Liao et al. (2010) implemented an automatic level-set technique for diagnosis of hematoma through multiple resolution binary images. Zaki et al. (2011) present a systematic approach for segmentation of Intracerebral hemorrhage (ICH) form CT images of brain. In their work the input CT images are segmented for deriving the region of abnormalities like hemorrhage through multi-level FCM followed by segmentation through two-level Otsu method (Kumar et al. 2013; Guo and Ashour 2019). These techniques are used as the basis for active contouring of the required region which can adopt two basic approaches like geometric and snake. Most segmentation techniques in practice run in interactive or semi-automatic manners and require manual intervention for adjusting parameters for segmentation by experienced radiologists (Neethu and Venkataraman 2015; Boers et al. 2013). Active contour models established on PDEs (Partial Differentiation Equations) or dynamic implicit interfaces are observed to be very effective for segmentation of medical images. Active contours were introduced by Kass et al. (1988) for object segmentation from images. Osher and Sethian in 1988 (Osher and Sethian 1988) introduced the level set theory for implementing the active contours. The various models associated with active contours are categorized into two classes Parametric and Geometric active contour (GAC). Parametric active contours (PAC) (Xu and Prince 1998) can be represented through Lagrangian framework as parameterized curves and geometric active contours can be characterized through Eulerian framework as level-sets. Caselles et al. (1997) presented a method for GACs implementation using level-set and curve evolution approach, in which initially the zero level-set function is used for representing the active contours that is evolved in accordance with PDE. GACs are preferred over parametric due to various advantages such as (*i*) geometric active contours can split and merge naturally while evolution which enables it to automatically handle topological changes and (*ii*) the level-set function is taken as fixed grid function.

Traditionally in level-set techniques, the nature of curve is kept smooth for the evaluation of level-set function near

to signed distance function (Peng et al. 1999). Thus, the traditional level-set methods periodically reinitializes the signed distance function during level-set evolution (Osher and Fedkiw 2006). The study (Kumar et al. 2020) presents entropy based unsupervised method for ICH segmentation on CT scan images. The work were evaluated using sensitivity, specificity, Dice coefficient, Jaccard index, precision and accuracy. the obtained results shows outstanding preformance.

However, as shown by Gomes and Faugeras in 2000 (Gomes and Faugeras 2000) reinitializing the level-set function violates the level-set method theory. Re-initialization is high pricey, complex and poses adverse side effects. To deal with these problems, in 2005, Li et al. (2005) presented a fast level-set design that forces its function close to a function called signed distance function that eradicates the requirement related with the expensive re-initialization process. The level-set function is initialized manually in majority of segmentation methods based on active contour. In the previous studies, it has also been found that fuzzy clustering methods were used for segmentation and provides the promising results (Bhadauria and Dewal 2014). In studies (Pratondo et al. 2017; Chen et al. 2019), active contour is used for the hemorrhage segmentation.

In recent scenario, deep learning based models are used for the image segmentation. The deep learning models are based on real time learning approach so that too much helpful in medical and health management system. There are so many studies based on deep learning model for image segmentation are mentioned in Chen et al. (2019); Saffari et al. (2018); Kooi et al. ((2017); Wang et al. (2016); Singh et al. (2020); Dhungel et al. (2015); Bellotti et al. (2006); Chang et al. (2018); Zhang (2021); Zhao et al. (2021); Wan and Lee (2020); Arora and Bhatia (2020); Hesamian et al. (2019); Zhong et al. (2021). In these previous studies benchmark datasets were used and attain the good quality result for either mass segmentation or mass detection or density segmentation.

In study (Hssayeni et al. 2020) shows the ICH segmentation using U-Net deep learning method on self collected dataset. The data augmentation were performed for creating more number of similar image using basic transformation techniques. The performed experiments were evaluated by the parameters Jaccard index, dice coefficient, sensitivity and specificity. The obtained value for respective parameters are 0.218, 0.315, 97.28% and 50.4%. Similar type of experiments were performed in study (Hu et al. 2020) on CT scan images using deep learning model.

The presented work proposes a segmentation method which first employs the fuzzy clustering method for level-set function initialization and then controls the evolution of this level-set function near the hemorrhage boundary, by estimating the evolution controlling parameters automatically from the image.

The manuscript is consisting of 7 sections. Section 2 describes the motivation behind the study and Sect. 3 illustrates the procedure followed in the proposed segmentation method to extract the hemorrhagic regions from CT images of brain, which briefly describes fuzzy clustering and level-set segmentation technique as these are utilized in proposed work. Section 4 illustrates material and performance evaluation parameters. Section 6 describes results and discussions associated with the proposed methods followed by conclusion and future expectations in Sect. 6 and Sect. 7, respectively.

2 Motivation of the work

Computer assisted biomedical image processing is very broad and widely used research topic for medical domain and there are so many studies found in the literature, where image processing is also used for organ segmentation. Among various imaging modalities CT scan is most prominent for human brain diagnosis and the results obtained from the fuzzy clustering is also commendable. The major motivation behind this work is taken from the medical experts who are facing difficulties is treatments. It has been noticed also that the identification of hemorrhagic area is very crucial due to its importance in diagnosis and planning related to treatment of hemorrhage. However, because of worst tissue contrast, the identification of hemorrhages using brain CT images becomes a challenging task. Due to this, Hemorrhage Detection using Edge-based Contour with Fuzzy Clustering using CT images are considered for this study.

3 Methodology

An approach that utilizes the features related to fuzzy clustering integrated with level-set method for segmenting the hemorrhage from CT images of brain has been presented in this paper. A brief illustration of fuzzy clustering and level-set methods have been discussed in sub-Sects. 2.1 and 2.2 respectively, the proposed method has been described in sub-Sect. 2.3.

3.1 Fuzzy clustering

Image segmentation aims at grouping the different intensity values represented by each pixel into various meaningful regions i.e. it partitions the image among c crisp regions {Ri} that are maximally connected and every *Ri* is consistent according to some criteria. Usually, it is difficult

to find whether or not a pixel is belonging to a region. In order to deal with such situation, segmentation process is done through fuzzy set concepts. FCM (Fuzzy C-mean) (Pal and (Ed.). 1992) is among the most preferred technique related to fuzzy clustering for segmentation of medical images. FCM partitions $\{x_k\}_{k=1}^{N}$ into clusters through minimization of objective function given as:

$$J = \sum_{i=1}^{c}\sum_{k=1}^{N} u_{ik}^{m}\|x_k - v_i\|^2 \tag{1}$$

Here x_k represents the gray value associated with k^{th} pixel, v_i represents ith cluster centre, u_{ik} represents fuzzy membership value of pixel k to cluster i and m denotes the fuzziness exponent with value above 1. Fuzzy membership must satisfy following constraints.

$$\sum_{i=1}^{c} u_{ik} = 1 \;\; \forall k; u_{ik} \in [0,1] \tag{2}$$

The u_{ik}(membership value) and v_i(cluster centers) associated with each pixel is evaluated iteratively as:

$$u_{ik} = \frac{\|x_k - v_i\|^{-2/m-1}}{\sum_{j=1}^{c}\|x_k - v_j\|^{-2/m-1}} \tag{3}$$

$$v_i = \frac{\sum_{k=1}^{N} u_{ik}^{m} x_k}{\sum_{k=1}^{N} u_{ik}^{m}} \tag{4}$$

FCM begins with randomly initializing the cluster centers which are iteratively converged to an optimal solution for vi which represents local minimum. The changes are observed at two consecutive iterations for membership value or center of clusters associated with each pixel which helps in determining the convergence, after this, defuzzification is done by assigning the clusters with the pixels having maximum membership values for that particular cluster.

3.2 Level set method (LSM)

Active contour methods are based on movement of the contour, subjected to constraints with respect to the given image. The contour starts over the object required for detection present in the image and advances to its interior normal unless it reaches the boundary. The LMS introduced by Osher and Sethian in 1988 (Osher and Sethian 1988), uses a 2D Lipschitz function as level-set function denoted by φ(x,y), representing contour C = {(x,y) / φ(x,y) = 0} which evolves through zero-level function given at time t as φ(t,x,y). The partial differential equation representing the evolution equation for level-set function is given as:

$$\frac{\partial\varphi}{\partial t} = |\nabla\varphi|F, \quad \varphi(0,x,y) = \varphi_0(x,y) \tag{5}$$

Here initial contour is represented by φ(0,x,y) and F denotes both the forces i.e. external and internal forces. A popular model for geometric active contour (Caselles et al. 1993) that utilizes mean curvature motion gives the formulation of level set function as:

$$\frac{\partial\varphi}{\partial t} = g|\nabla\varphi|\left(div\left(\frac{\nabla\varphi}{|\nabla\varphi|}\right) + v\right) \tag{6}$$

where ν represents a constant called artificial balloon force, g represents edge function used for stopping level set evolution near the optimal solution. Instance g is evaluated as:

$$g = \frac{1}{1 + |\nabla G_\sigma(x,y) * u_0(x,y)|^2} \tag{7}$$

Here u_0 represents given image, Gσ* u0 is the smoother version of u0 and Gσ represents smoothing Gaussian function having standard deviation σ.

The major challenge in level-set is regarding its function (φ) which needs to be reinitialized periodically assigned distance function. Practically, the re-initialization operation can be costly, might contain side-effects and is cumbersome. For dealing with the re-initialization issue, Li et al. (2005) introduced variational level-set method which entirely eradicates the requirement of re-initialization. This formulation is given as:

$$\frac{\partial\varphi}{\partial t} = \mu\left[\Delta\varphi - div\left(\frac{\nabla\varphi}{|\nabla\varphi|}\right)\right] + \lambda\delta(\varphi)div\left(g\frac{\nabla\varphi}{|\nabla\varphi|}\right) + vg\delta(\varphi) \tag{8}$$

In the above equation, the first term known as regularization term is associated with internal energy and it forces the level-set function denoted as φ to automatically reach to the signed distance function. The second term and the third term are known as length and balloon force term respectively, associated with energy function's gradient flows and are also responsible to drive the zero-level contours toward the object boundary. μ represents weighting coefficient of regularization term, λ represents weighting coefficient related to length term and ν represents balloon force. δ(x) is Dirac function and in practice it is slightly smoothed as δε(x).

$$\delta_\varepsilon(z) = \begin{cases} 0, & |z| > \varepsilon \\ \frac{1}{2\varepsilon}\left[1 + \cos(\frac{\pi z}{\varepsilon})\right], & |z| \le \varepsilon \end{cases} \tag{9}$$

Here ε represents constant that regularized the Dirac function.

Here, the initialization of level-set function φ_0(x,y) is performed as:

$$\varphi_0(x,y) = \begin{cases} c, & (x,y) \in \Omega \\ -c, & (x,y) \notin \Omega \end{cases} \tag{10}$$

where c denotes a constant that must be greater than 2ε and Ω represents the initial contour such that $\varphi_0(x,y) > 0$. This procedure has eliminated the re-initializing process.

The discretization of Eq. (8) is expressed in iteration form as:

$$\varphi_{x,y}^{t+1} = \varphi_{x,y}^{t} + \tau \frac{\partial \varphi_{x,y}^{t}}{\partial t} \tag{11}$$

where τ represents time step parameter, that could be taken adequately large. The μ (penalty term) and τ (time step parameter) should satisfy τ.μ < ¼ in order to maintain the stable evaluation of level-set.

3.3 Proposed segmentation method

The proposed approach employs the features of fuzzy clustering as well as level-set method for segmenting the area of hemorrhage present within the CT image of brain. In proposed technique the fuzzy clustering is utilized for initializing the level-set function. It can be noticed that the FCM generates spurious blobs along with the outliers within the image. These side-effects are detached with the help of morphological operations like dilation and erosion. The erosion operation helps dealing with these issues through shrinking and removing the spurious blobs as well as the outliers present in image, and the dilation helps through expanding and recovering the object of interest.

After performing these morphological operations, the initialization of level-set function is done through the results yielded from the fuzzy clustering. Let Ui,j = [Ui,j] represent the membership function related to fuzzy segmentation. The binary image Zi,j contains the object of interest is then extracted from the input image, such that

$$Z_{i,j} = \begin{cases} 1, & u_{i,j} \geq b_0 \\ 0, & otherwise \end{cases} \tag{12}$$

$b_0 \in (0, 1)$ represents the adjustable threshold.

Now using the above mentioned equation, the initialization of level-set function is done as:

$$\varphi_0(x,y) = 2\varepsilon(2Z_{i,j} - 1) \tag{13}$$

Here ε represents a constant meant for regularizing the Dirac function as given Eq. (9). In the conventional level-set methods various controlling parameters are input manually with values varying with respect to required application, in order to control the evolution of level-set function. In this proposed method, all the required controlling parameters are adaptively evaluated through results yielded from fuzzy segmentation. The area along with length associated with the contour produced through fuzzy clustering are evaluated by utilizing the Heaviside and Dirac function respectively as

$$C_{Area}(\varphi \geq 0) = \int_{\Omega} H(\varphi(x,y))dxdy \tag{14}$$

$$C_{length}(\varphi = 0) = \int_{\Omega} \delta_0(\varphi(x,y))|\nabla\varphi(x,y)|dxdy \tag{15}$$

Here Heaviside function can be defined as:

$$H(\varphi) = \begin{cases} 1, & if\ \varphi \geq 0 \\ 0, & if\ \varphi < 0 \end{cases} \tag{16}$$

and the Dirac function as:

$$\delta_0(\varphi) = \frac{d}{d\varphi} H(\varphi) \tag{17}$$

As Li et al. (2005) proposed in 2005, time step (τ) related with evolution of level-set in Eq. (11) can be selected with adequately large value. Moreover, the product of this τ and μ (regularization coefficient) should satisfy τ.μ < ¼ for achieving stable evolution. This time step parameter τ can be calculated as:

$$\tau = \frac{C_{Area}}{C_{Length}} \tag{18}$$

The μ (regularization coefficient) is evaluated as:

$$\mu < \frac{1}{4\tau} \tag{19}$$

From the experiments it is observed that larger value of λ approaches smoother contour and the larger value of ν speeds up the evolution of contour towards the object's boundaries. Thus λ is taken as:

$$\lambda = 0.5/\mu \tag{20}$$

The balloon force ν generates the attraction of level-set function towards the region that is to be extracted. The balloon force can either shrink or expand the level-set function depending on the sign of ν; thus, it eradicates the requirement of initializing the level-set function close to the required object's boundaries. The value of ν shows the pressure and it is observed that it must be larger enough to pass through spurious edges. Therefore in the proposed method value of ν is determined from the results produced through fuzzy segmentation as:

$$\nu = 0.5 - u_{i,j} \tag{21}$$

where $u_{i,j}$ represents value of membership function associated with fuzzy segmentation for every pixel contained within an image.

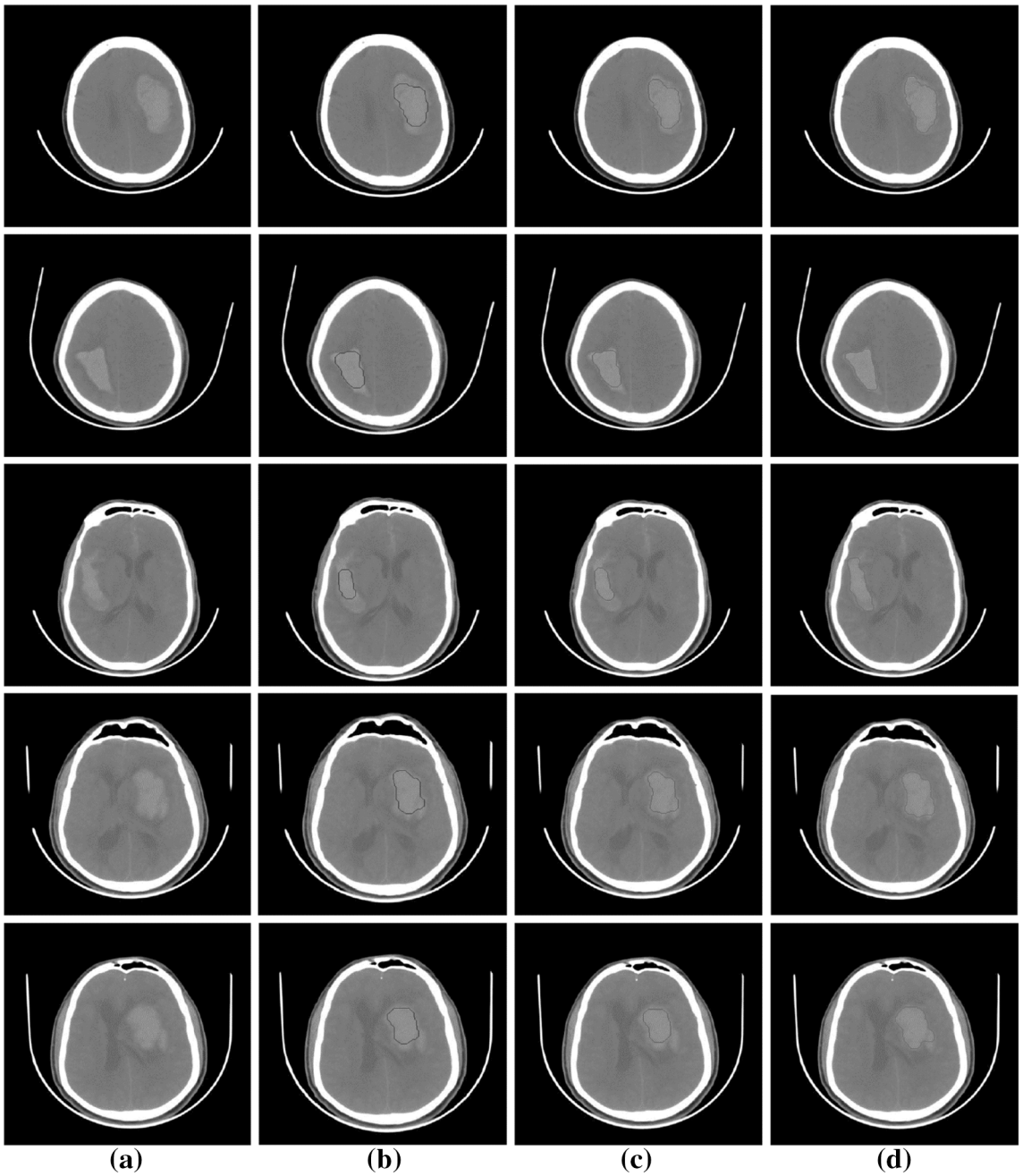

Fig. 2 Hemorrhage contours: Column (**a**) Original CT images (**b**) Region growing (**c**) Fuzzy clustering (**d**) Proposed method

4 Dataset and performance evaluation

4.1 Dataset description

For evaluating the proposed segmentation technique performances, dataset containing 300 haemorrhagic CT images of brain is collected. The GE medical systems CT scanner has been used for obtaining the given CT images of brain with field of view as 25 × 25 cm and the peak tube current and tube voltage of 100 mA and 120 kV respectively. The size of each of these images is 512 × 512 pixels, which results a resolution per pixel of 0.49 × 0.49 mm^2. The thickness of slice and inter slice space are 3 mm and 7 mm respectively.

4.2 Performance evaluation parameters

For the evaluation, the haemorrhage regions are manually outlined by the expert of respective subject, and have considered as ground truth. The quantitative analysis of the

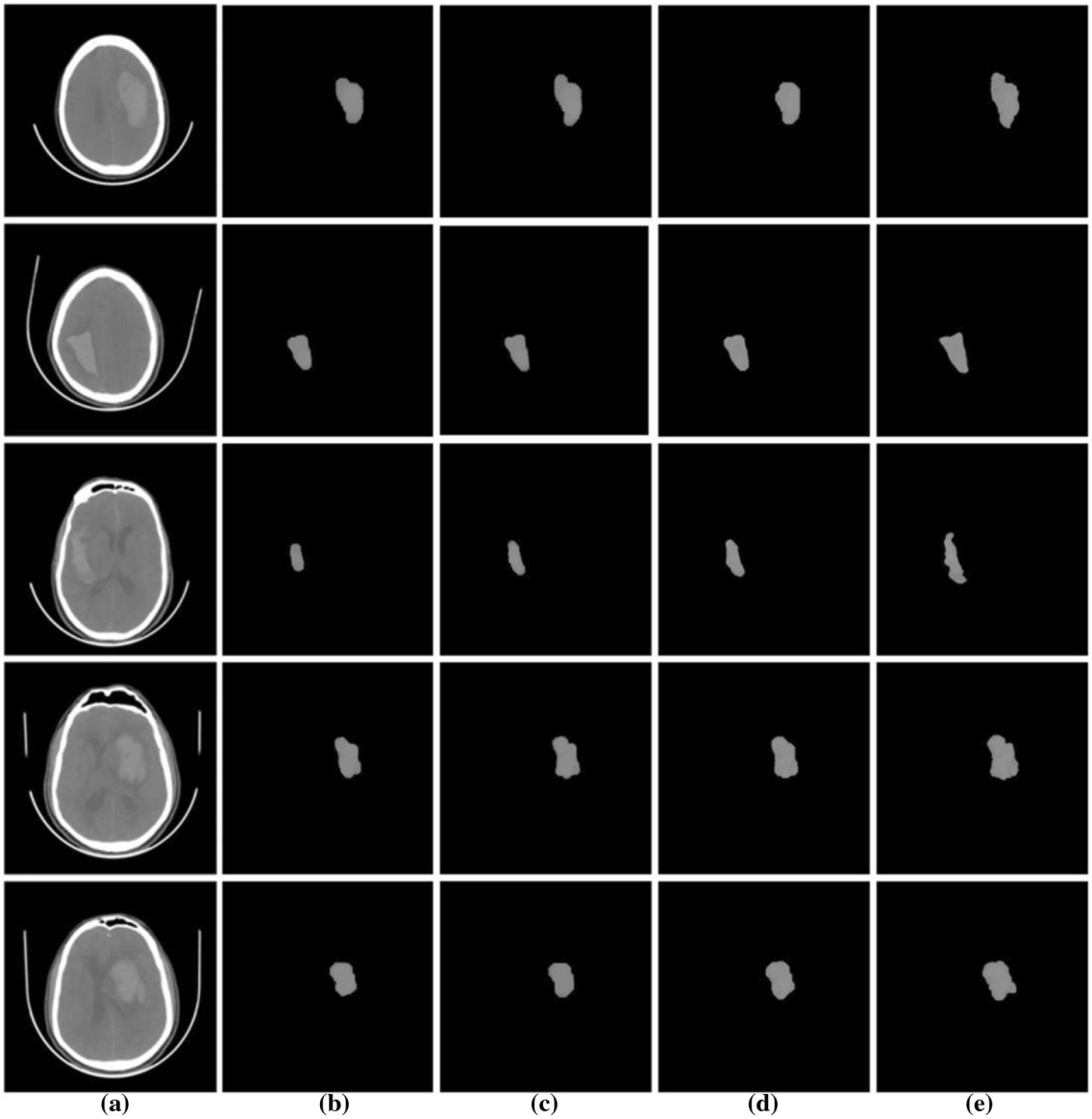

Fig. 3 Segmentation result: Column (**a**) Input CT image (**b**) Hemorrhage region marked by expert (**c**) Hemorrhage region detected by region growing (**d**) Hemorrhage region detected by Fuzzy clustering (**e**) Hemorrhage region detected by Proposed method

performance associated with the proposed technique is done through the ground truth-based parameters such as overlap metric, accuracy, specificity and sensitivity. Sensitivity in percentage refers to the number of pixels which have been correctly segmented for haemorrhagic region out of all segmented pixels. Specificity in percentage defines the number of pixels that have properly been excluded from segmented haemorrhagic region out of all the pixels that are excluded from haemorrhagic region of ground truth image. Accuracy is simply the ratio of pixels that are segmented as haemorrhagic region in output image to the number of pixels present in ground truth haemorrhagic region. These parameters can be evaluated as

$$\%Overlap = \left(\frac{2 * TP}{2 * TP + FP + FN}\right) * 100 \tag{22}$$

$$\%Sensitivity = \left(\frac{TP}{TP + FN}\right) * 100 \tag{23}$$

$$\%Specificity = \left(\frac{TN}{TN + FP}\right) * 100 \tag{24}$$

$$\%Accuracy = \left(\frac{TP + TN}{TP + TN + FP + FN}\right) * 100 \tag{25}$$

TP or True Positive represents the pixels belonging to the haemorrhagic region in output image which are also present in that region in ground truth image. TN or True Negative signifies the pixels which do not belong to

Table 1 Comparison of haemorrhagic area in CT images of brain obtained through different techniques

CT scan no	Hemorrhagic area (cm^2)						
	MD (a)	RG (b)	Difference (a−b)	FC (c)	Difference (a−c)	Proposed (d)	Difference (a−d)
1	16.72	13.68	3.04	14.55	2.17	15.03	1.69
2	11.87	7.97	3.9	9.42	2.45	9.64	2.23
3	10.78	8.62	2.16	8.99	1.79	9.33	1.45
4	16.62	12.7	3.92	13.43	3.19	14.78	1.84
5	15.44	13.95	1.49	13.83	1.61	13.92	1.52
6	17.09	14.74	2.35	15.34	1.75	15.58	1.51
7	11.08	7.74	3.34	9.25	1.83	9.6	1.48
8	11.52	7.18	4.34	9.65	1.87	9.94	1.58
9	12.46	9.16	3.3	10.64	1.82	10.66	1.8
10	15.48	13.95	1.53	13.85	1.63	13.98	1.5
11	12.52	8.22	4.3	10.63	1.89	12.93	0.41
12	10.87	6.97	3.9	8.42	2.45	9.19	1.68
13	11.4	8.16	3.24	9.6	1.8	9.72	1.68
14	12.09	8.74	3.35	9.24	2.85	9.74	2.35
15	15.62	11.65	3.97	12.35	3.27	12.91	2.71
16	14.09	10.01	4.08	13.15	0.94	14.34	0.25
17	9.78	6.58	3.2	7.99	1.79	8.21	1.57
18	10.12	8.82	1.3	8.69	1.43	10.17	0.05
19	10.14	8.82	1.32	8.62	1.52	9.23	0.91
20	13.09	11.12	1.97	12.14	0.95	13.25	0.16
21	1.72	1.22	0.5	1.28	0.44	1.36	0.36
22	11.48	9.16	2.32	9.2	2.28	9.43	2.05
23	1.58	1.18	0.4	1.32	0.26	1.42	0.16
24	9.53	6.61	2.92	7.53	2	7.81	1.72
25	12.36	8.72	3.64	8.52	3.84	9.07	3.29
Average	11.82	9.03	**2.79**	9.91	**1.91**	10.45	**1.44**

MD Manually delineated, *RG* Region growing, *FC* Fuzzy clustering

haemorrhagic region in computerised as well as ground truth image. FP or False Positive represents pixels that are present in haemorrhagic region's border of output image but is absent in same region of ground truth image. FN or False Negative represents pixels absent in haemorrhagic region's border of output image but is present in the same region of ground truth image (Metz 1978).

5 Experimental results and discussion

In this experimentation, the proposed method for segmentation has been implemented on a dataset consisting 300 images, out of which the segmentation results on 5 images have been shown in Fig. 2. The results produced through proposed segmentation method are compared with Region Growing (RG) and Fuzzy Clustering (FC) based segmentation methods.

In Fig. 2, columns (b)–(d) show the final contours of the hemorrhages extracted by various segmentation methods i.e. RG, FC, and proposed method respectively. The visual results in Fig. 2 show that the proposed method has higher accuracy in extracting the haemorrhagic regions as compared with other techniques. The sample image of segmented haemorrhagic regions are shown in Fig. 3.

In Fig. 3, Column (a) is used to represent the input images and column (b–e) are used for the segmented region by expert, region growing, Fuzzy clustering and proposed method, respectively. A total of three experts have been participated for ground truth region segmentation and all of them have more than 15 years of experience in brain CT Hemorrhage detection.

Table 1 show the area of hemorrhagic regions extracted using the proposed algorithm and state-of-the-art techniques and their comparative assessment with respect to the

Table 2 Analysis of sensitivity and specificity associated with haemorrhage area detected through various methods on CT images

Image no	Sensitivity			Specificity		
	Region growing	Fuzzy clustering	Proposed method	Region growing	Fuzzy clustering	Proposed method
1	74.79	78.85	85.59	98.67	99.93	99.77
2	85.63	85.18	90.26	97.74	99.13	99.44
3	58.95	75.63	76.49	99.66	99.52	93.91
4	76.89	77.25	77.76	99.67	99.68	99.48
5	65.24	71.92	72.35	90.62	86.89	99.97
6	62.2	73.46	73.19	99.45	99.94	100
7	82.84	84.56	87.27	99.65	99.72	99.74
8	64.91	77.73	80.15	99.64	99.23	99.9
9	58.86	76.17	78.74	96.45	92.29	96.89
10	57.89	68.84	69.85	99.56	100	99.91
11	62.2	73.16	74.57	99.4	99.93	99.77
12	57.89	67.84	70.33	99.59	100	100
13	74.59	78.95	84.67	98.66	99.91	99.92
14	62.18	71.02	72.3	90.6	86.89	92.28
15	58.9	74.75	78.24	99.76	99.55	99.75
16	53.86	78.17	81.34	96.47	92.2	96.88
17	85.53	85.01	87.49	97.75	99.12	98.36
18	83.81	84.58	86.71	99.68	99.71	99.71
19	76.61	77.15	80.27	99.57	99.58	99.27
20	60.83	77.77	80.64	99.64	99.09	100
21	71.32	72.34	75.61	99.56	99.32	99.32
22	77.19	71.56	74.15	99.77	100	99.02
23	83.05	81.92	87.11	99.41	99.59	99.23
24	79.92	85.07	85.64	98.33	99.21	98.15
25	82.49	86.39	86.91	99.58	99.26	98.97
Average	70.34	77.41	**79.91**	98.36	97.99	**98.79**

area of same region present in ground truth images for randomly selected 25 CT images.

The hemorrhagic regions identified through proposed method lies within the range of 1.36 cm2 and 15.58 cm^2 with a mean value of 10.45 cm^2 for randomly selected 25 CT images from a dataset of 300 CT images of brain. The averages of differences between the haemorrhagic areas identified through the FC and RG, and the ground truth area are 1.91 and 2.79 respectively. While the value for same identified through proposed technique is 1.44 that is minimum. It shows that the segmented results yielded through proposed method closely resembles with ground truth. Thus, it can be observed that the proposed method has outperformed all the other aforesaid methods in terms of accurately segmenting the hemorrhage from CT images of brain.

The quantitative assessment of segmentation results produced through the proposed method has been done using similarity indices i.e. overlap, accuracy, specificity and sensitivity evaluated for randomly selected 25 CT images from a dataset of 300 CT images of brain, have been shown in Tables 2 and 3. For proposed technique, the sensitivity ranges from 69.85 to 90.26 with a mean value as 79.91 and specificity ranges from 92.28 to 100 with a mean value as 98.79. For further validation, overlap and accuracy metric have also been evaluated. The accuracy lies in the range from 76.09 to 95.21 with a mean value as 85.40 and overlap lies in the range from 75.70 to 93.16 with a mean value as 87.46. It is clear from Tables 2 and 3 that average values associated with every similarity indices taken in this work on a randomly selected 25 CT images from a dataset of 300 CT images of brain for proposed method that means the results produced through proposed method correlate well with measurements done by the experts.

Based on the above observations, it is illustrated that the proposed method for segmentation has significantly improved the results related with segmentation of haemorrhage in terms of similarity indices mentioned earlier.

Table 3 Measurement of accuracy and overlap evaluated for hemorrhage detection techniques on CT images of brain

Image no	Accuracy			Overlap		
	RG	FC	Proposed	RG	FC	Proposed
1	82.56	86.87	89.57	86.42	88.10	91.12
2	84.52	84.67	85.78	91.44	91.49	93.16
3	88.85	94.32	95.21	74.29	85.34	85.14
4	76.26	76.82	79.14	86.44	86.87	87.01
5	82.88	83.19	85.09	77.68	78.14	80.53
6	74.20	72.14	79.02	77.69	84.48	88.87
7	83.59	84.24	85.44	91.25	91.75	91.90
8	75.82	77.63	80.91	76.65	87.15	90.44
9	85.24	92.99	93.00	70.63	84.05	88.12
10	78.87	77.82	79.70	73.43	80.54	83.04
11	82.19	83.11	84.16	76.69	84.47	83.62
12	87.89	87.84	89.90	73.33	80.84	83.42
13	74.56	78.88	85.41	85.43	88.19	90.45
14	72.18	72.79	76.09	76.68	77.14	80.51
15	78.85	74.41	81.53	74.09	85.33	85.66
16	82.24	83.99	86.27	68.63	85.05	87.80
17	84.15	84.27	86.87	91.40	91.46	92.77
18	83.57	84.34	87.12	91.05	91.50	91.36
19	76.06	76.82	77.52	86.40	86.89	86.94
20	80.83	87.07	88.20	75.65	87.05	89.86
21	84.42	88.73	91.70	81.60	87.41	91.53
22	85.04	84.20	85.64	82.46	81.30	83.78
23	89.79	89.90	91.23	88.64	88.78	90.73
24	91.04	92.82	90.75	90.20	92.33	92.99
25	77.37	75.49	79.68	70.93	71.81	75.70
Average	81.72	83.01	85.40	80.76	85.50	87.46

This shows, the proposed segmentation method segments the haemorrhagic area present within the CT images of brain with greater accuracy.

6 Conclusion

Brain hemorrhage is one of the least curable type of strokes and has maximum rate of mortality. Due to such high rate of morbidity and mortality, the frequency of hemorrhage detection is imperative for clinician, and so CT imaging, which is more rapid and cost effective than other imaging modalities, is still utilized as the gold standard for the preliminary evaluation of the brain haemorrhage. On the other hand, due to weak boundaries, worst tissue contrast and intensity inhomogeneities, it becomes difficult for an expert to detect the haemorrhage from CT images. In this paper, a segmentation method for detecting hemorrhage has been proposed that employs the characteristics of both, the edge-based active contour as well as the fuzzy clustering, for CT images of brain. The strength of proposed technique for segmentation has been tested on dataset comprising of 300 CT images of brain. From the experimental results, it is concluded that this proposed technique is more robust as well as precise for recognizing the hemorrhagic regions. The outcomes produced by the proposed method closely resemble the ground truth images of experts as well as their measurements. The proposed system is expected to be beneficial for patient's care particularly during the time of emergency as crucial decision making is required which consumes time.

7 Future expectation and limitations

The extensive work has been further carried for brain hemorrhage detection or segmentation using fully automated level-set method and also with the help of semantic image segmentation and deep learning models like DeepLab, Segnet, DCNN etc. The same work has been also carried for the future work as the impact of denoising algorithm on CT image for brain hemorrhage detection or segmentation. This would be also considered as a limitation of the current study. But the inclusion of denoising methods, the system complexity is increased and it will take more time to process the images. Therefore denoising methods are not included in the study. But it can be considered for the future study.

Acknowledgements The authors are grateful to TEQIP-III of Uttarakhand Technical University, Dehradun, for providing financial and technical support under advice No.- C081908384733. Further authors are greatly indebted towards Graphic era hill university and CCET Chandigarh for providing necessary support to carry out this work also the flexibility provided by the university to researchers is highly appreciable.

Funding No funding.

Declarations

Conflict of interest This article does not contain any studies with human participants or animals performed by any of the authors.

References

Al-Ayyoub M, Alawad D, Al-Darabsah K, Aljarrah I (2013) Automatic detection and classification of brain hemorrhages. WSEAS Trans Comput 12(10):395–405

Arora S, Bhatia MPS (2020) Presentation attack detection for iris recognition using deep learning. Int J Syst Assur Eng Manag 11:232–238. https://doi.org/10.1007/s13198-020-00948-1

Bardera A, Boada I, Feixas M, Remollo S, Blasco G, Silva Y, Pedraza S (2009) Semi-automated method for brain hematoma and

edema quantification using computed tomography. Comput Med Imaging Graph 33(4):304–311
Bellotti R, De Carlo F, Tangaro S, Gargano G, Maggipinto G, Castellano M, Massafra R, Cascio D, Fauci F, Magro R, Raso G (2006) A completely automated CAD system for mass detection in a large mammographic database. Med Phys 33(8):3066–3075
Bhadauria HS, Dewal ML (2014) Intracranial hemorrhage detection using spatial fuzzy c-mean and region-based active contour on brain CT imaging. SIViP 8(2):357–364
Boers AM, Marquering HA, Jochem JJ, Besselink NJ, Berkhemer OA, van der Lugt A, Beenen LF, Majoie CB (2013) Automated cerebral infarct volume measurement in follow-up noncontrast CT scans of patients with acute ischemic stroke. Am J Neuroradiol 34(8):1522–1527
Caselles V, Catté F, Coll T, Dibos F (1993) A geometric model for active contours in image processing. Numer Math 66(1):1–31
Caselles V, Kimmel R, Sapiro G (1997) Geodesic active contours. Int J Comput Vision 22(1):61–79
Chan T (2007) Computer aided detection of small acute intracranial hemorrhage on computer tomography of brain. Comput Med Imaging Graph 31(4–5):285–298
Chang PD, Kuoy E, Grinband J, Weinberg BD, Thompson M, Homo R, Chen J, Abcede H, Shafie M, Sugrue L, Filippi CG (2018) Hybrid 3D/2D convolutional neural network for hemorrhage evaluation on head CT. Am J Neuroradiol 39(9):1609–1616
Chen L, Bentley P, Rueckert D (2017) Fully automatic acute ischemic lesion segmentation in DWI using convolutional neural networks. NeuroImage: Clinical. 15:633–643
Chen, Y., Chen, G., Wang, Y., Dey, N., Sherratt, R.S. and Shi, F., 2019. A Distance Regularized Level-set Evolution Model Based MRI Dataset Segmentation of Brain's Caudate Nucleus. *IEEE Access*.
Cohen WA (1992) Computed tomography of intracranial hemorrhage. Radiologic Clin North Amer 2:75–87
Dhungel, N., Carneiro, G. and Bradley, A.P., 2015, November. Automated mass detection in mammograms using cascaded deep learning and random forests. In *2015 international conference on digital image computing: techniques and applications (DICTA)* (pp. 1–8). IEEE. techniques and applications (DICTA) 2015 Nov 23 (pp. 1–8). IEEE.
Gillebert CR, Humphreys GW, Mantini D (2014) Automated delineation of stroke lesions using brain CT images. NeuroImage: Clinical. 4:540–548
Gomes J, Faugeras O (2000) Reconciling distance functions and level sets. J vis Commun Image Represent 11(2):209–223
Guo, Y., & Ashour, A. S. 2019. Neutrosophic sets in dermoscopic medical image segmentation. In *Neutrosophic Set in Medical Image Analysis* (pp. 229–243). Academic Press. https://doi.org/10.1016/B978-0-12-818148-5.00011-4
Heron MP (2019) Deaths: leading causes for 2017. Natl Vital Stat Rep 68(6):1–77
Hesamian MH, Jia W, He X et al (2019) deep learning techniques for medical image segmentation: achievements and challenges. J Digit Imaging 32:582–596. https://doi.org/10.1007/s10278-019-00227-x
Hssayeni MD, Croock MS, Salman AD, Al-khafaji HF, Yahya ZA, Ghoraani B (2020) Intracranial hemorrhage segmentation using a deep convolutional model. Data 5(1):14
Hu K, Chen K, He X, Zhang Y, Chen Z, Li X, Gao X (2020) Automatic segmentation of intracerebral hemorrhage in CT images using encoder–decoder convolutional neural network. Inf Process Manag. 57(6):102352
Kass M, Witkin A, Terzopoulos D (1988) Snakes: active contour models. Int J Comput Vision 1(4):321–331
Kooi T, Litjens G, Van Ginneken B, Gubern-Mérida A, Sánchez CI, Mann R, den Heeten A, Karssemeijer N (2017) Large scale deep learning for computer aided detection of mammographic lesions. Med Image Anal 35:303–312
Kumar S, Kumar P, Sharma TK et al (2013) Bi-level thresholding using PSO, artificial bee Colony and MRLDE embedded with Otsu method. Memetic Comp 5:323–334. https://doi.org/10.1007/s12293-013-0123-5
Kumar I, Bhatt C, Singh KU (2020) Entropy based automatic unsupervised brain intracranial hemorrhage segmentation using ct images. J King Saud Univ-Comput Inf Sc. https://doi.org/10.1016/j.jksuci.2020.01.003
Li, C., Xu, C., Gui, C. and Fox, M.D., 2005, June. Level set evolution without re-initialization: a new variational formulation. In *2005 IEEE Computer Society Conference on Computer Vision and Pattern Recognition (CVPR'05)* (Vol. 1, pp. 430–436). IEEE.
Liao CC, Xiao F, Wong JM, Chiang IJ (2010) Computer-aided diagnosis of intracranial hematoma with brain deformation on computed tomography. Comput Med Imaging Graph 34(7):563–571
Loncaric, S., Kovacevic, D. and Cosic, D., 1998, May. Fuzzy expert system for edema segmentation. In *MELECON'98. 9th Mediterranean Electrotechnical Conference. Proceedings (Cat. No. 98CH36056)* (Vol. 2, pp. 1476–1479). IEEE.
Loncaric, S., Dhawan, A.P., Cosic, D., Kovacevic, D., Broderick, J. and Brott, T., 1999, May. Quantitative intracerebral brain hemorrhage analysis. In *Medical Imaging 1999: Image Processing* (Vol. 3661, pp. 886–894). International Society for Optics and Photonics.
Metz, C.E., 1978, October. Basic principles of ROC analysis. In *Seminars in nuclear medicine* (Vol. 8, No. 4, pp. 283–298). WB Saunders. DOI=10.1.1.692.1962.
Murphy SL, Xu J, Kochanek KD, Arias E, Tejada-Vera B (2021) Deaths: final Data for 2018. Natl Vital Stat Rep 69(13):1–83
Neethu, S. and Venkataraman, D., 2015. Stroke detection in brain using CT images. In *Artificial Intelligence and Evolutionary Algorithms in Engineering Systems* (pp. 379–386). Springer, New Delhi.
Osher, S. and Fedkiw, R., 2006. *Level set methods and dynamic implicit surfaces* (Vol. 153). Springer Science & Business Media.
Osher S, Sethian JA (1988) Fronts propagating with curvature-dependent speed: algorithms based on Hamilton-Jacobi formulations. J Comput Phys 79(1):12–49
Pal, S. K. (Ed.). 1992. *Fuzzy models for pattern recognition: methods that search for structures in data*. Institute of Electrical & Electronics Engineers (IEEE Press).
Peng D, Merriman B, Osher S, Zhao H, Kang M (1999) A PDE-based fast local level set method. J Comput Phys 155(2):410–438
Pratondo A, Chui CK, Ong SH (2017) Integrating machine learning with region-based active contour models in medical image segmentation. J vis Commun Image Represent 43:1–9
Praveen GB, Agrawal A, Sundaram P, Sardesai S (2018) Ischemic stroke lesion segmentation using stacked sparse autoencoder. Comput Biol Med 99:38–52
Saffari, N., Rashwan, H.A., Herrera, B., Romani, S., Arenas, M. and Puig, D., 2018, October. On Improving Breast Density Segmentation Using Conditional Generative Adversarial Networks. In *CCIA* (pp. 386–393).
Sethian J (1999) Level set methods and fast marching method. Cambridge University Press
Singh SP, Wang L, Gupta S, Gulyás B, Padmanabhan P (2020) Shallow 3D CNN for detecting acute brain hemorrhage from medical imaging sensors. DOI, IEEE Sens J. https://doi.org/10.1109/JSEN.2020.3023471
Suri, J.S., Singh, S. and Laxminarayan, S., 2002. Medical image segmentation using level sets. In *PDE and level sets: algorithmic*

approaches to static and motion imagery (pp. 301–340). Springer, Boston, MA.

Wan W, Lee HJ (2020) Deep feature representation and ball-tree for face sketch recognition. Int J Syst Assur Eng Manag 11:818–823. https://doi.org/10.1007/s13198-019-00882-x

Wang J, Yang X, Cai H, Tan W, Jin C, Li L (2016) Discrimination of breast cancer with microcalcifications on mammography by deep learning. Sci Rep 6:27327

Xu C, Prince JL (1998) Snakes, shapes, and gradient vector flow. IEEE Trans Image Process 7(3):359–369

Yezzi A, Kichenassamy S, Kumar A, Olver P, Tannenbaum A (1997) A geometric snake model for segmentation of medical imagery. IEEE Trans Med Imaging 16(2):199–209

Zaki WMDW, Fauzi MFA, Besar R, Ahmad WSHMW (2011) Abnormalities detection in serial computed tomography brain images using multi-level segmentation approach. Multimedia Tools Appl 54(2):321–340

Zhang X (2021) Application of human motion recognition utilizing deep learning and smart wearable device in sports. Int J Syst Assur Eng Manag. https://doi.org/10.1007/s13198-021-01118-7

Zhang Y, Brady M, Smith S (2001) Segmentation of brain MR images through a hidden Markov random field model and the expectation-maximization algorithm. IEEE Trans Med Imaging 20(1):45–57

Zhao X, Chen K, Wu G, Zhang G, Zhou X, Lv C, Yao Z (2021) Deep learning shows good reliability for automatic segmentation and volume measurement of brain hemorrhage, intraventricular extension, and peripheral edema. Eur Radiol. https://doi.org/10.1007/s00330-020-07558-2

Zhong X, Amrehn M, Ravikumar N, Chen S, Strobel N, Birkhold A, Maier A (2021) Deep action learning enables robust 3D segmentation of body organs in various CT and MRI images. Sci Rep 11(1):1–14. https://doi.org/10.1038/s41598-021-82370-6